SUB-Y-TYPE ANTENNA ARRAY CONFIGURATION FOR HIGH RESOLUTION INTERFEROMETRIC SYNTHETIC APERTURE RADIOMETER

Gum-Sil Kang, Jiang Jingshan* ,Yong-Hoon Kim,

Kwangju Institute of Science and Technology (K-JIST)

1 Oryong-dong, Buk-gu, Gwangju, 500-712, Korea

Tel: +82-62-970-2387, Fax: +82-62-970-2384, Email: yhkim@kjist.ac.kr

***Center for Space Science and Applied Research, Chinese Academy of Sciences**

ABSTRACT

The development of 2-D radiometer is a new technical challenge for space borne remote sensing area. The Y-type antenna array has been proposed as a most efficient configuration because a large alias free FOV and a small-synthesized beam-width can be achieved compared to L-, T-type under the fixed antenna spacing. New configuration of antenna array, which is called sub-Y type configuration, is proposed to obtain a higher angular resolution than the case of Y-type array in the paper. The sub-Y type array is consisted of basic arrays, which are the Y-type array of four antenna elements. To analyze characteristics of the proposed configuration, the synthesized beam pattern is simulated through simulation. The secondary effect of the sub-Y-type is that the reconstructed image is suffered from the alias effect is appeared around the real target. The ghost targets in the reconstructed image can be reduced by the alias suppression algorithm introduced in this paper. In conclusion, the performance evaluation by use of array factor simulation shows more than 37.5 % improvement in average for angular resolution and almost similar performance for temperature resolution.

I. INTRODUCTION

Interferometric synthetic aperture radiometers have been developed to obtain a high angular resolution using a static array of small antennas, avoiding the scanning of the large size antenna required by real aperture radiometer [1][2]. ESTAR is a radiometer combining real aperture in one dimension and synthetic aperture in the other, and the airborne demonstration model has been built by the University of Massachusetts at Amherst under NASA grant [1]. 2-D interferometric radiometer such as MIRAS uses a 2-D array of small antennas and its imaging characteristics depend on a type of antenna array because a brightness temperature image is indirectly generated from a sampled visibility function. Y-type antenna array has been proposed as a most efficient configuration because a large FOV and a narrow synthesized beamwidth can be achieved compared to other type of configuration when the number of antenna elements is fixed and the antenna spacing is constant [2]. In this paper sub-Y type configuration is proposed to obtain a wider coverage of sampled visibility function than Y-type array configuration. The interferometric measurement for synthetic aperture radiometer is introduced briefly to discuss the imaging characteristics of the sub-Y-type configuration. Fig. (1) shows the geometry of interferometric measurement for aperture synthesis. If the antennas, the amplifiers, filters and correlators are identical, and the baseband brightness process has suffered little decorrelation between the two antennas, the complex correlation output $V(u,v)$ is given by [1]

$$V(u,v) = \iint_{\zeta^2+\eta^2 \le 1} T_B(\zeta,\eta) \exp[-j2\pi(u\zeta + v\eta)]\, d\zeta\, d\eta \quad (1)$$

where $u = D_x/\lambda$, $v = D_y/\lambda$, $\zeta = \sin\theta\cos\phi$, $\eta = \sin\theta\sin\phi$ and λ is the wavelength of the incident radiation at the antennas. The visibility function $V(u,v)$, which is a spatial frequency spectrum of the brightness temperature distribution $T_B(\zeta,\eta)$, is sampled by complex cross correlation between the output signals of two separated antennas on the measurement plane.

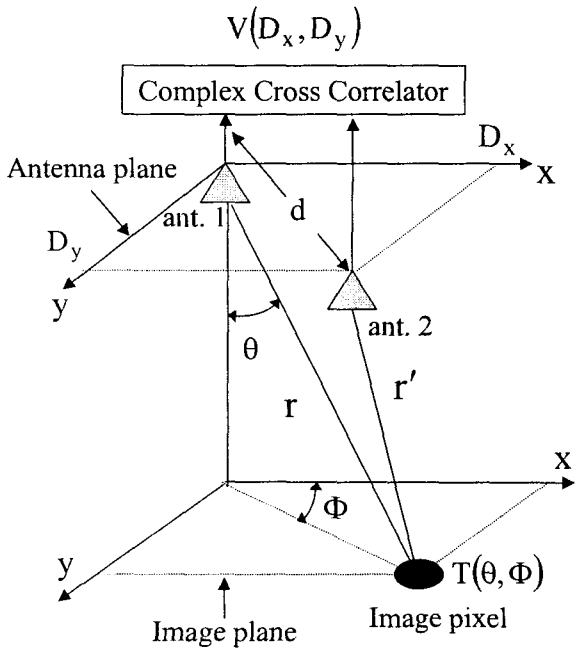

Figure 1. Geometry of interferometric measurement.

The discrete visibility samples are collected from all of possible pairs of two antennas on a static array and the estimated brightness temperature distribution $\hat{T}_B(\zeta,\eta)$ is reconstructed by the discrete 2-D IFFT given by

$$\hat{T}_B(\zeta,\eta) = \sum_u \sum_v W(u,v)\, V(u,v) \exp[j2\pi(u\zeta + v\eta)] \quad (2)$$

where $W(u,v)$ means the weight function used to decrease the sidelobe level.

II. SUB-Y-TYPE CONFIGURATION AND ITS VISIBILITY FUNCTION SAMPLING

In this section the sub-Y-type array configuration that is designed for the use of 2-D high angular resolution interferometric synthetic aperture radiometer system is introduced. For the development of interferometric radiometer system, the design of the antenna array configuration is important because the synthesized beam pattern is mainly affected with the type of the antenna array. 2-D antenna array configuration such as T-, L- and Δ-, Y-type has been used for a 2-D synthetic aperture radiometer [2]. Y-type antenna array has been proposed as a most efficient configuration because a large FOV and a narrow synthesized beamwidth can be achieved compared to other type of configuration when the number of antenna elements and the antenna spacing are fixed [2]. The synthesized 3 dB beamwidth of an interferometric synthetic aperture radiometer is reduced proportionally to the coverage area of the sampled visibility function because a brightness temperature image is indirectly generated by FT(Fourier Transform) of sampled visibility function. The sub-Y-type array configuration is devised to obtain wider coverage area than the conventional Y-type array keeping the hexagonal sampling characteristic under the fixed antenna element.

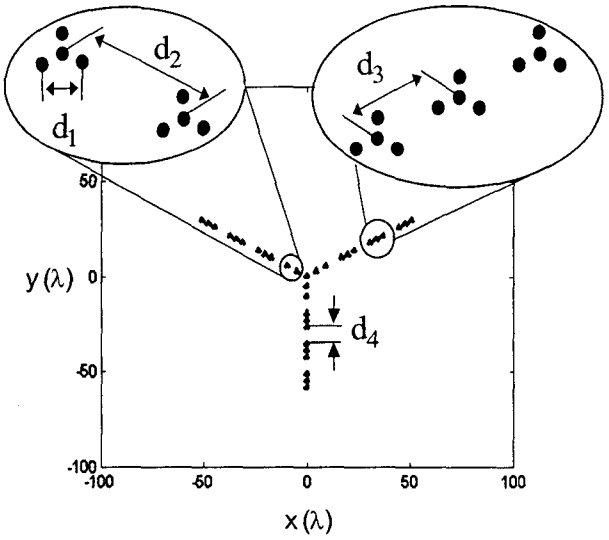

Figure 2. Sub-Y-type array configuration

To describe the sub-Y-type array, let defines a basic array that consists of a small number of antenna elements than the total elements of a whole array. The basic array can be designed as various types such as Y-type, linear array and triangle type array. The entire shape of sub-Y-type

array is Y-type that does not consist of single antenna elements but basic arrays. The antenna space of basic array is selected to satisfy a required alias-free FOV like as the case of conventional Y-type. The spacing between basic arrays is extended to obtain a wide coverage area of visibility sample. The distribution of sampled visibility functions on coverage area depends on the arrangement of the basic arrays. Fig 2 shows the sub-Y-type array configuration with four elements Y-type basic array. The antenna spacing of the basic array is presented by d_1. The basic arrays located at center, first basic array and second basic array on each arm are arranged at d_2. Three of basic arrays that are located at constant distance d_3 are grouped as one unit and these units are located at regular spacing d_4.

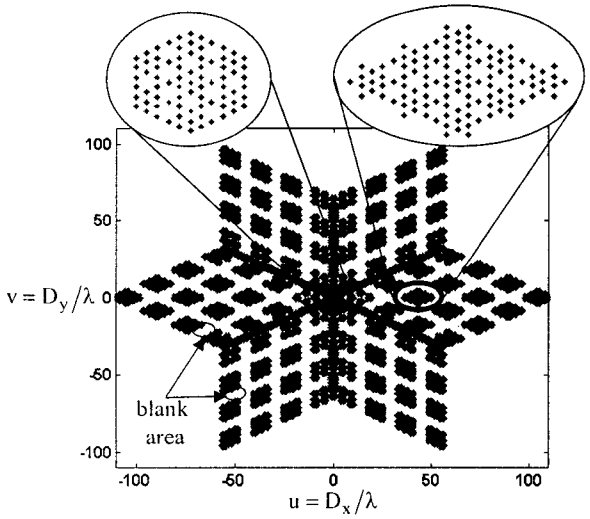

Figure 3. Visibility function sampling of sub-Y-type

The shape of coverage, the sampling grid and the sample spacing including the coverage area are important sampling characteristics of visibility function because these factor affects on the reconstructed brightness image. These sampling characteristics depend on the type of array, the number of antenna elements and antenna spacing. The sampling characteristics of sub-Y-type array are a little different from the conventional array type. The visibility sampling depends on the type of basic array and spacing between basic arrays including antenna spacing and the number of antenna elements. The spacing between basic arrays is extended to obtain the visibility function on wider coverage area than the case of conventional Y-type under the fixed number of antenna elements. For sub-Y-type configuration the visibility functions are sampled over the hexagonal grid on the star shape of coverage area like as conventional Y-type. The different sampling characteristic from the case of the conventional Y-type is that the visibility functions are not sampled every sampling point on the coverage area. In Fig 3 the visibility functions are obtained on a small star coverage area because of Y-type basic array. There are un-sampled region between these small star coverage on the whole coverage area because the basic arrays are located sparsely. The redundancy of sampled visibility function is depends on the type of basic array. While the redundancies fall only on the three principal axes in the case Y-type array, for the sub-Y-type array the redundancies shown by Fig. 4 appear in the whole coverage area.

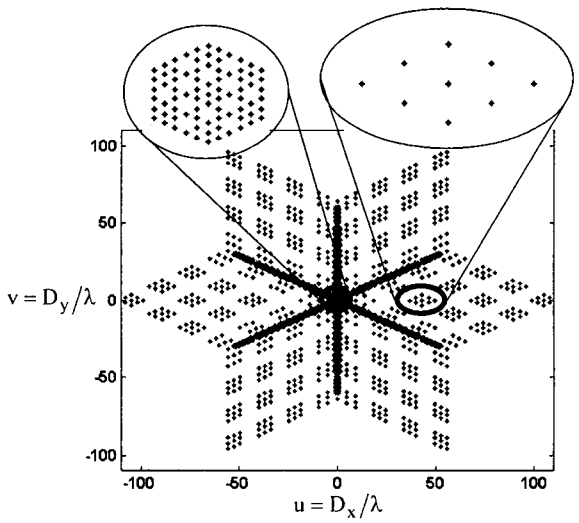

Figure 4. Redundancy of visibility function sample of sub-Y-type

III. IMAGING CHARACTERISTICS OF SUB-Y-TYPE ARRAY CONFIGURATION

The general imaging characteristic of sub-Y-type configuration is discussed in this section. Simulation result to analyze the imaging characteristics of sub-Y-type array is presented in Fig 5. This synthesized beam shows different pattern from the case of conventional

antenna configuration such as X-, T-, L-, Y-type because of different sampling characteristics.

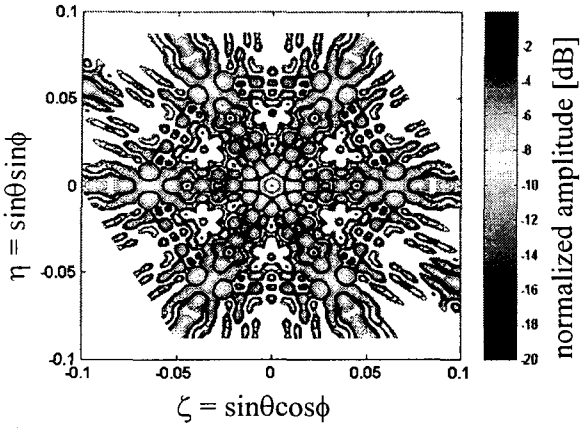

(a) 2-D pattern of synthesized beam

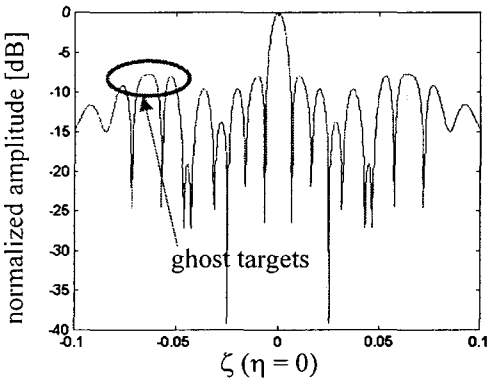

(b) 1-D pattern of synthesized beam

Figure 5. Synthesized beam pattern for sub-Y-type array (d_1=0.89λ, d_3=4 d_1, $d_2 = d_4$=12 d_1)

When the sub-Y-type configuration is used, the narrow synthesized beam is achieved by extending the spacing between the basic arrays. Another important imaging characteristic is that there are ghost targets at about –7 dB level around the main beam on the reconstructed beam pattern. This bad effect is due to the un-sampled region on the coverage area of visibility function. The distribution of ghost targets is changed as the spacing between the basic arrays. The synthesized beam pattern for different spacing between basic arrays in Fig. 1 is simulated to analyze general imaging characteristics of sub-Y-type under the fixed number of antenna elements 136. Table 1 shows the characteristics of synthesized beam pattern as to the spacing between the basic arrays when the rectangular window is applied. When the spacing between the basic arrays is extended, the 3 dB beam width narrowed and the ghost target enlarged.

Table 1. Characteristics of synthesized beam pattern (Total number of antenna elements: 136)

	3 dB beam width	SLL	Maximum alias level
Conventional Y-type			
antenna spacing = 0.89λ	0.75°	-7.6 dB	-
Sub-Y-type d_1=0.89λ, d_3=4 d_1			
$d_2 = d_4$=18 d_1	0.32° (57.3%)	-7.6 dB	-5.1 dB
$d_2 = d_4$=16 d_1	0.35° (53.3%)	-7.7 dB	-5.5 dB
$d_2 = d_4$=14 d_1	0.38° (49.3%)	-7.7 dB	-5.9 dB
$d_2 = d_4$=12 d_1	0.43° (42.7%)	-7.9 dB	-6.6 dB
$d_2 = d_4$=10 d_1	0.49° (34.7%)	-8.0 dB	-7.7 dB
$d_2 = d_4$=8 d_1	0.55° (26.7%)	-7.9 dB	-7.8 dB
$d_2 = d_4$=6 d_1	0.63° (16.0%)	-7.6 dB	-8.9 dB

IV. ALIAS SUPPRESSION ALGORITHM FOR SUB-Y-TYPE CONFIGURATION

For the sub-Y-type configuration the incomplete sampling of visibility functions on the coverage area causes the alias effect on the reconstructed image and it deteriorate the image quality. The alias suppression algorithm to remove this alias effect is briefly introduced in this section. This algorithm is based on the 1-D profile of sampled visibility function. The brightness temperature image $\hat{T}_B(\zeta,\eta)$ can be expressed in terms of 1-D profile $\hat{T}_B\_N_2(k_1,n_2)$ like as (5) through the coordinate transformation by (3), (4). Also the standard FFT algorithm can be used for image reconstruction by this coordinate transformation [3][4]. For simplicity, the window function is assumed as a rectangular window function in (6).

$$\begin{bmatrix} u \\ v \end{bmatrix} = d \begin{bmatrix} \frac{\sqrt{3}}{2} & 0 \\ -\frac{1}{2} & 1 \end{bmatrix} \begin{bmatrix} k_1 \\ k_2 \end{bmatrix} \tag{3}$$

where $k_1,k_2 = 0,1,2,...,N_T$ and N_T is the total sampling number of visibility function.

$$\begin{bmatrix}\zeta\\ \eta\end{bmatrix}=\frac{1}{N_T d}\begin{bmatrix}\frac{1}{\sqrt{3}} & \frac{2}{\sqrt{3}}\\ 1 & 0\end{bmatrix}\begin{bmatrix}n_1\\ n_2\end{bmatrix} \quad (4)$$

where $n_1, n_2 = 0, 1, 2, \ldots, N_T$.

$$\hat{T}_B(n_1,n_2)=\sum_{k_1}\hat{T}_B\_N_2(k_1,n_2)\exp[-j2\pi\frac{k_1 n_1}{N_T}] \quad (5)$$

$$\hat{T}_B\_N_2(k_1,n_2)=\sum_{k_2}V(k_1,k_2)\exp[-j2\pi\frac{k_2 n_2}{N_T}] \quad (6)$$

If the number of visibility function samples over k_2 is constant, the amplitude responses of $\hat{T}_B\_N_2(k_1,n_2)$ for all of k_1 are exactly same. Therefore for sub-Y-type configuration shown in Fig. 2 the alias free 1-D profile $\hat{T}_B\_N_2(k_1,n_2)\big|_{k_1=0}$ can be used as a reference profile to remove the alias effect of $\hat{T}_B\_N_2(k_1,n_2)$. Also the alias-free 1-D profile $\hat{T}_B\_N_1(n_1,k_2)\big|_{k_2=0}$ can be used as the reference profile for $\hat{T}_B\_N_1(n_1,k_2)$. These reference profiles are expressed in equation (9) and (11).

$$F_{N_1}(n_1)=\hat{T}_B\_N_1(n_1,k_2)\big|_{k_2=0} \quad (8)$$

$$=\sum_{k_1}V(k_1,0)\exp[-j2\pi\frac{k_1 n_1}{N_T}] \quad (9)$$

$$F_{N_2}(n_2)=\hat{T}_B\_N_2(k_1,n_2)\big|_{k_1=0} \quad (10)$$

$$=\sum_{k_2}V(0,k_2)\exp[-j2\pi\frac{k_2 n_2}{N_T}] \quad (11)$$

Equation (12) – (15) show the method to remove the alias effects of the original 1-D profiles by use of the reference profile.

$$\left|\tilde{T}_B\_N_2(k_1,n_2)\right|=\sqrt{\left|\hat{T}_B\_N_2(k_1,n_2)\right|\times\left|F_{N_2}(n_2)\right|} \quad (12)$$

$$\angle\tilde{T}_B\_N_2(k_1,n_2)=\angle\hat{T}_B\_N_2(k_1,n_2) \quad (13)$$

$$\left|\tilde{T}_B\_N_1(n_1,k_2)\right|=\sqrt{\left|\hat{T}_B\_N_1(n_1,k_2)\right|\times\left|F_{N_1}(n_1)\right|} \quad (14)$$

$$\angle\tilde{T}_B\_N_1(n_1,k_2)=\angle\hat{T}_B\_N_1(n_1,k_2) \quad (15)$$

When this algorithm is applied, the synthesized beam pattern presented in Fig. 5 is changed to the beam pattern like as Fig. 6. The beam pattern broadened a little, but the maximum alias level decreased to about –16 dB level when the rectangular window is used. The 3dB beamwidth is narrow more than 0.47° and it is reduced to 37.5 % of that of the conventional Y-type configuration. The first sidelobe level is similar to the value of the conventional Y-type.

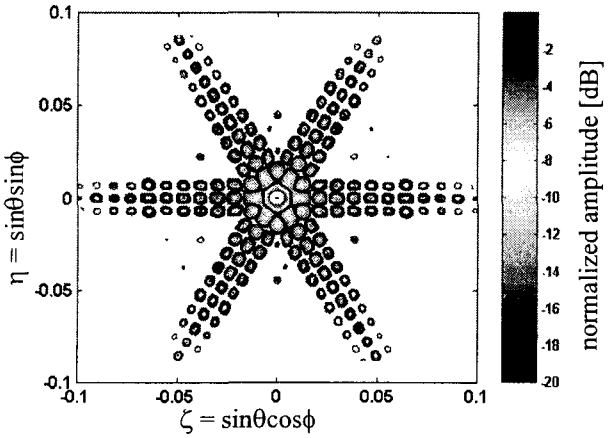

(a) 2-D pattern of synthesized beam

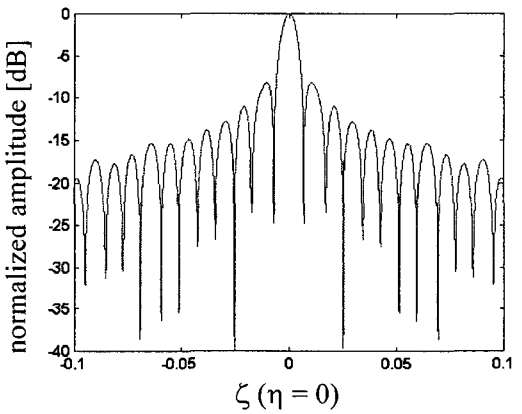

(b) 1-D beam pattern of synthesized beam

Figure 6. Synthesized beam pattern for sub-Y-type array when the alias suppression algorithm is applied.
(d_1=0.89λ, d_3=4 d_1, $d_2 = d_4$=12 d_1)

V. CONCLUSION

The imaging characteristics of the sub-Y-type configuration are analyzed through the simulation of synthesized beam. When 136 antenna elements are used, using the sub-Y-type configuration presented at Fig. 2 that is arranged by the antenna spacing of d_1=0.89λ, d_3=4 d_1 and $d_2 = d_4$=12 d_1, the 3 dB beamwidth is reduced to 42.7 % of that of the conventional Y-type. The side lobe level is similar to the case of conventional Y-type. The alias suppression algorithm is proposed to remove the alias effect caused by the un-sampled region on the coverage area. The alias free 1-D profiles at k_1 = 0 and k_2 = 0 are used as reference filters to suppress the alias effect. After the alias suppression algorithm is applied, the maximum alias level decrease to about –16 dB and the synthesized beamwidth broadened a little. Still, it is reduced to 37.5 % of that of the conventional Y-type.

VI. ACKNOWLEDGEMENT

This work was supported in part by the KOREA Science and Engineering Foundation (KOSEF) through the Advanced Environmental Monitoring Research Center at Kwangju Institute of Science and Technology and the international collaboration program with Center for Space Science and Applied Research (CSSAR) funded by MOST. The authors wish to acknowledge Prof. Jiang from CSSAR.

REFERENCE

[1] Christoper S. Ruf, Calvin T. Swift, Alan B. Tanner 1998. Interferometric Synthetic Aperture Microwave Radiometry for the Remote Sensing of the Earth, IEEE Transactions on geoscience and remote sensing, Vol. 26, No. 5, pp. 597-611.

[2] J. Bara, A. Camps 1998. Angular resolution of two-dimensional, hexagonally sampled interferometric radiometers, Radio Science, Vol. 33, Number 5, September-October, pp.459-1473.

[3] James C. Ehrhardt, 1993. Hexagonal Fast Fourier Transform with Rectangular Output, IEEE Transactions on signal processing, Vol. 41, No. 3, March, pp. 1469-1472.

[4] Russell M. Mersereau, 1979. The Processing of Hexagonally Sampled Two-Dimensional Signals, Proceeding of the IEEE, Vol. 67, No. 6, June, pp.930-949.